Neuron
Article

Evoked Axonal Oxytocin Release in the Central Amygdala Attenuates Fear Response

H. Sophie Knobloch,[1,4] Alexandre Charlet,[2,4] Lena C. Hoffmann,[1] Marina Eliava,[1,3] Sergey Khrulev,[1,5] Ali H. Cetin,[1,6] Pavel Osten,[1,7] Martin K. Schwarz,[1] Peter H. Seeburg,[1] Ron Stoop,[2,*] and Valery Grinevich[1,*]
[1]Department of Molecular Neurobiology, Max Planck Institute for Medical Research, Heidelberg 69120, Germany
[2]Centre for Psychiatric Neuroscience, Department of Psychiatry, University Hospital Center Lausanne, Prilly-Lausanne CH-1008, Switzerland
[3]Department of Clinical Neurobiology, German Cancer Research Institute, Heidelberg 69120, Germany
[4]These authors contributed equally to this work
[5]Present address: Leibniz Institute for Molecular Pharmacology, Berlin 10117, Germany
[6]Present address: Systems Neurobiology Laboratory, The Salk Institute for Biological Studies, La Jolla, CA 92037, USA
[7]Present address: Cold Spring Harbor Laboratory, Cold Spring Harbor, NY 11724, USA
*Correspondence: rstoop@unil.ch (R.S.), valery.grinevich@mpimf-heidelberg.mpg.de (V.G.)
DOI 10.1016/j.neuron.2011.11.030

SUMMARY

The hypothalamic neuropeptide oxytocin (OT), which controls childbirth and lactation, receives increasing attention for its effects on social behaviors, but how it reaches central brain regions is still unclear. Here we gained by recombinant viruses selective genetic access to hypothalamic OT neurons to study their connectivity and control their activity by optogenetic means. We found axons of hypothalamic OT neurons in the majority of forebrain regions, including the central amygdala (CeA), a structure critically involved in OT-mediated fear suppression. In vitro, exposure to blue light of channelrhodopsin-2-expressing OT axons activated a local GABAergic circuit that inhibited neurons in the output region of the CeA. Remarkably, in vivo, local blue-light-induced endogenous OT release robustly decreased freezing responses in fear-conditioned rats. Our results thus show widespread central projections of hypothalamic OT neurons and demonstrate that OT release from local axonal endings can specifically control region-associated behaviors.

INTRODUCTION

Oxytocin (OT) is an evolutionarily ancient neuropeptide found in species ranging from invertebrates to mammals (Donaldson and Young, 2008). In mammals, the major sources of OT are the hypothalamic paraventricular (PVN), supraoptic (SON), and accessory magnocellular nuclei (AN) (Sofroniew, 1983; Swanson and Sawchenko, 1983). Axons of the vast majority of OT neurons and vasopressin (VP) neurons terminate in the posterior lobe of the pituitary, forming the classic hypothalamic-neurohypophyseal system (Brownstein et al., 1980). From the posterior pituitary, OT reaches the general blood circulation and acts on target organs, exerting uterine contraction and milk ejection from the mammary glands.

Besides these well-known neuroendocrine effects, OT attracts increasing interest for its effects in the forebrain, affecting fear, trust, and other social behaviors (Lee et al., 2009). OT exerts powerful anxiolytic effects (Neumann, 2008) in the central nucleus of amygdala (CeA), the core brain structure underlying fear responses (Hitchcock and Davis, 1991; Kapp et al., 1979; Wilensky et al., 2006). In the lateral CeA (CeL), local application of OT activates a subpopulation of GABAergic interneurons that inhibits neurons in the medial CeA (CeM), the main output of the CeA to the brainstem (Huber et al., 2005), thereby attenuating behavioral fear responses (Viviani et al., 2011).

Although these behavioral effects of OT are well documented, the pathway through which OT reaches the amygdala and other forebrain regions and its precise cellular origins still remain unknown. Systemic OT cannot pass the blood-brain barrier (McEwen, 2004), and hence, there must be central OT release. The prevailing hypothesis over the last 20 years has been that central OT function is mediated by dendritic OT release in the hypothalamus, followed by passive diffusion to various brain structures (Landgraf and Neumann, 2004; Ludwig and Leng, 2006; Veenema and Neumann, 2008). However, OT receptors (OT-R; Gimpl and Fahrenholz, 2001) occur throughout the brain at various distances from the hypothalamus, and hence, passive diffusion would put severe limitations on the time course and specificity of OT signaling. Such limitations could be overcome by long-range axonal projections of hypothalamic OT neurons (Ross and Young, 2009).

To resolve this important outstanding issue in the field, we sought evidence for axonal OT-containing processes of hypothalamic origin that demonstrate functional OT release. To visualize OT axons, we selectively expressed fluorescent marker proteins from an OT gene promoter by infecting hypothalamic neurons with a recombinant adeno-associated virus (rAAV). Expression and activation of rAAV-directed channelrhodopsin-2 (ChR2; Nagel et al., 2003) in OT neurons revealed that blue light

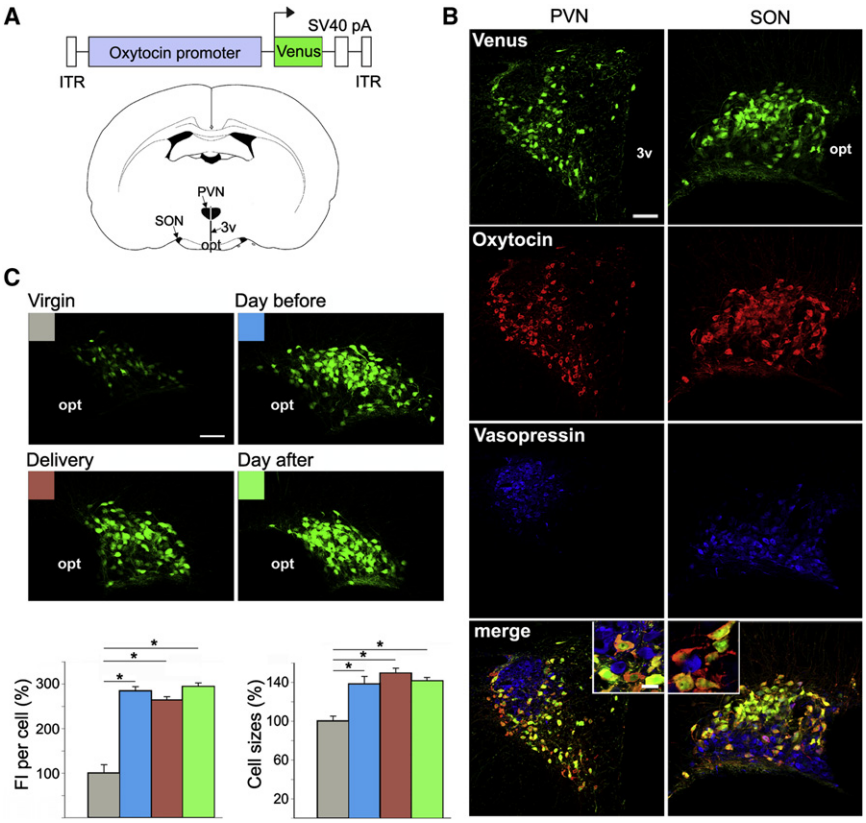

Figure 1. Cell-Type Specificity of Virally Infected OT Neurons

(A) An rAAV-expressing Venus under the control of a 2.6 kb mouse OT promoter was injected into PVN and SON of adult female rats.

(B) Viral infection resulted in Venus expression in OT, but not VP, neurons.

(C) Increased intrinsic Venus fluorescence intensity (FI) and sizes of cell bodies in the SON on the day before delivery (blue), day of delivery (orange) and day after delivery (green) compared to virgin rats (gray), as presented in graphs below. *$p < 0.01$. Scale bars represent 50 μm in (B) and (C) and 10 μm in insets in (B). 3v, third ventricle; opt, optic tract.

triggered, in vitro, an OT-receptor-mediated increase in neuronal activity in the CeL, enhanced the frequency of inhibitory postsynaptic currents (IPSCs) in the CeM, and decreased, in vivo, context-evoked freezing responses in fear-conditioned rats. Our findings provide direct evidence for local, endogenous OT signaling in the suppression of CeA-mediated fear (Roozendaal et al., 1992a, 1992b; Viviani et al., 2011).

RESULTS

Specificity of Virus-Directed Gene Expression in Neurons of the Rat Hypothalamus

We constructed an rAAV-expressing Venus from a 2.6 kb region upstream of OT exon 1 (Figure 1A) and conserved in mammalian species (see Experimental Procedures). The injection of this rAAV into the PVN or SON of rats (Figure 1A) resulted in the selective expression of Venus in OT, but not VP, neurons (Figure 1B). Quantitative analysis in the SON, PVN, and AN of virgin and lactating rats showed more than 97% colocalization of OT and Venus expression and only 1.70% ± 0.36% of Venus-positive neurons expressing VP, revealing a very efficient and highly specific virus expression (Table 1).

The virally introduced OT promoter appears to be regulated during late pregnancy (Zingg and Lefebvre, 1988) and lactation (Burbach et al., 2001), like its chromosomal counterpart. We indeed found a 3-fold increase in fluorescent intensity, as well as larger sized green fluorescent OT cells around delivery compared to virgin rats (Figure 1C), in accordance with earlier studies (Theodosis, 2002). Despite these differences in size and Venus expression, we found no significant changes in the absolute numbers of identified OT neurons (Table 1).

Efferent Projections from Hypothalamic OT Neurons to Forebrain Structures

In view of these important differences in OT expression, we used lactating rats to reveal the fine, thin projections of OT axonal arbors in the forebrain (see Figure S1 available online). OT neurons of the PVN and SON projected to a wide range of OT-R-expressing forebrain structures (Figures 2 and S2; Gimpl and Fahrenholz, 2001), though PVN neurons provided many more prominent projections to more numerous structures (29 of 34 regions analyzed; Figure 2) than SON neurons (five regions; see Figure S2 for quantification). Previous studies reported high OT-R expression and OT-R-mediated effects in the CeA, a structure critically involved in the expression of conditioned fear (Huber et al., 2005; Bosch et al., 2005). We found Venus-positive processes from the PVN to engulf and enter the CeA but only marginally observed single Venus-positive processes from the SON, mostly at the ventrolateral CeA (Figures 3 and S2). In animals targeted in all OT nuclei, including AN, we observed significantly more Venus-positive fibers in the CeA, preferentially located in the CeL (Figures 3A and S3). These contained OT-positive puncta (Figure 3B), confirming their exclusive origin from OT neurons (see Figure S3 for quantification).

Cytochemical Markers in CeA Projections from Hypothalamic OT Neurons

At the light microscopic level, the small-diameter, branching, and en passant varicosities of Venus-positive processes suggested that the above-observed fibers were axons. To corroborate their axonal nature, we expressed in OT neurons the axonal marker Tau tagged by enhanced green fluorescent protein (EGFP). We observed an EGFP signal in all fibers within the CeA and in axonal terminals in the posterior pituitary (Figure 3C).

Table 1. Quantification of OT-Promoter Specificity in OT-ergic Nuclei in the Hypothalamus of Virgin and Lactating Rats. Results are Presented as Percentage ± SEM.

Animals	Comparison	SON	PVN	rSON	CN	DLN
Virgin Rats	OT versus Venus	99.57% ± 0.66%	99.8% ± 0.49%	99.07% ± 2.27%	98.48% ± 3.71%	98.47% ± 2.59%
		n = 1,091	n = 936	n = 115	n = 69	n = 210
	Venus versus OT	98.01% ± 3.09%	97.34% ± 2.03%	98.13% ± 2.97%	97.57% ± 3.82%	97.66% ± 2.15%
		n = 1,091	n = 936	n = 115	n = 69	n = 210
Lactating Rats	OT versus Venus	100%	99.57% ± 0.85%	100%	100%	99.56% ± 1.07%
		n = 987	n = 969	n = 116	n = 74	n = 207
	Venus versus OT	99.06% ± 1.48%	99.06% ± 2.3%	100%	100%	99.55% ± 1.10%
		n = 987	n = 969	n = 116	n = 74	n = 207

n, absolute number of identified neurons per structure and condition; CN, circular nucleus; DLN, dorsolateral nucleus; rSON, retrochiasmatic part of the SON.

Similarly, expression of a synaptophysin-EGFP fusion protein revealed synaptic terminals in both structures (Figure 3D). Costaining of synaptophysin-EGFP puncta with antibodies against OT and vesicular glutamate transporter 2 (VGluT2), the mRNA of which was detected in OT neurons (Kawasaki et al., 2005), demonstrated overlap of EGFP, VGluT2, and OT signals (Figure 3E), confirming previous reports on magnocellular neurons enriched by microvesicles that associate with synaptophysin (Navone et al., 1989) and contain glutamate (Meeker et al., 1991). Higher-resolution electron microscopic analysis revealed the presence of synaptic contacts between immunoreactive axon terminals and local dendrites in the CeL (Figure 3F), most likely dendrites of GABAergic interneurons, of which the CeL is predominantly composed (Davis, 2000; Huber et al., 2005). In the three cases analyzed, we encountered synaptic appositions bearing the features of asymmetric (Gray's type 2) synapses, proposed to be of excitatory nature (Figure 3F). Importantly, we were unable to find synaptic contacts within the CeM (M.E., unpublished data), where fibers are traversing the region without branching and forming varicosities, as was the case in the CeL (Figure S3A). Our collective findings strongly suggest a presence in the CeL of axonal terminals that originate from OT neurons and form glutamatergic synapses.

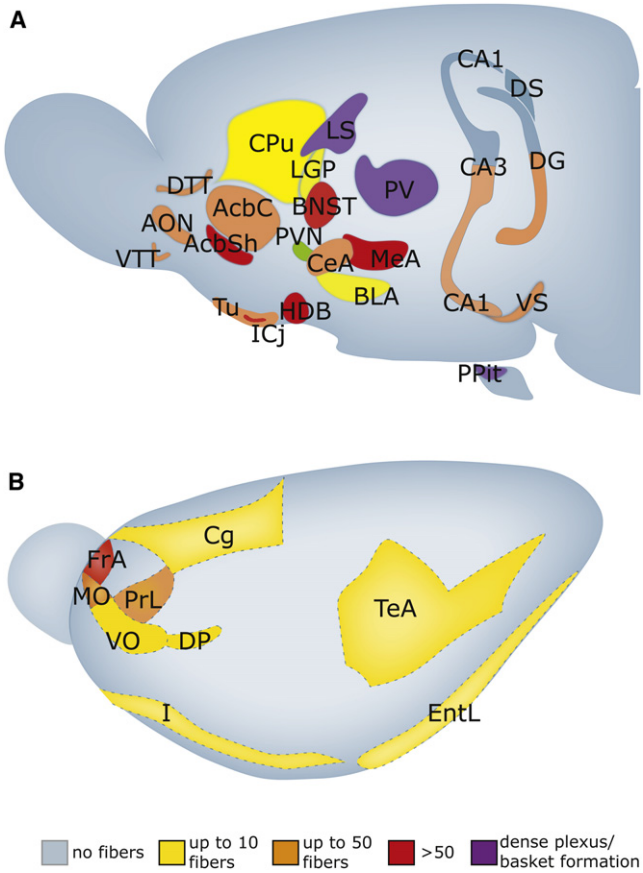

Figure 2. Distributions of Venus-Labeled OT Fibers from the PVN in Extrahypothalamic Forebrain Regions of Lactating Rats

(A and B) OT/GFP fiber pattern in subcortical (A) and cortical (B) areas. The infected PVN in one hemisphere is colored in green. The density of fibers is depicted in the following colors: yellow, orange, red, and violet. The detailed information on forebrain projections from ipsi- and contralateral PVN and SON, as well as examples of stained GFP fibers, are presented in Figure S2. For abbreviations of structures, see Figure S2.

Blue-Light Activation of ChR2-Expressing Axons In Vitro Induces Local OT Release

Based on the anatomical evidence for OT-containing axonal fibers of hypothalamic origin in the CeA, we selectively expressed the blue-light (BL)-sensitive ChR2 protein (Nagel et al., 2003) fused to mCherry (Figure 4A) in all hypothalamic OT neurons via an rAAV. Whole-cell voltage-patch-clamp recordings in vitro in coronal slices of mCherry fluorescent cells (Figures 4A and 4B, top) revealed functional ChR2 expression in PVN, SON, and AN neurons, as evident from the presence of BL induced currents with a characteristic rapidly inactivating peak followed by a stable tail (Boyden et al., 2005; Figures 4C and S4). Because high frequencies of action potentials are thought to be necessary to trigger release of neuropeptides, in contrast to release of classical neurotransmitters (Hökfelt, 1991), we quantified the effect of different BL stimulations on AP frequencies of PVN and SON neurons. Current-clamp recordings from these neurons showed that AP frequencies up to 20 Hz could be reliably induced by stimulation frequencies with short BL pulses of 10 ms applied at 30 Hz, as well as by continuous BL exposure (Figures 4C and S4A).

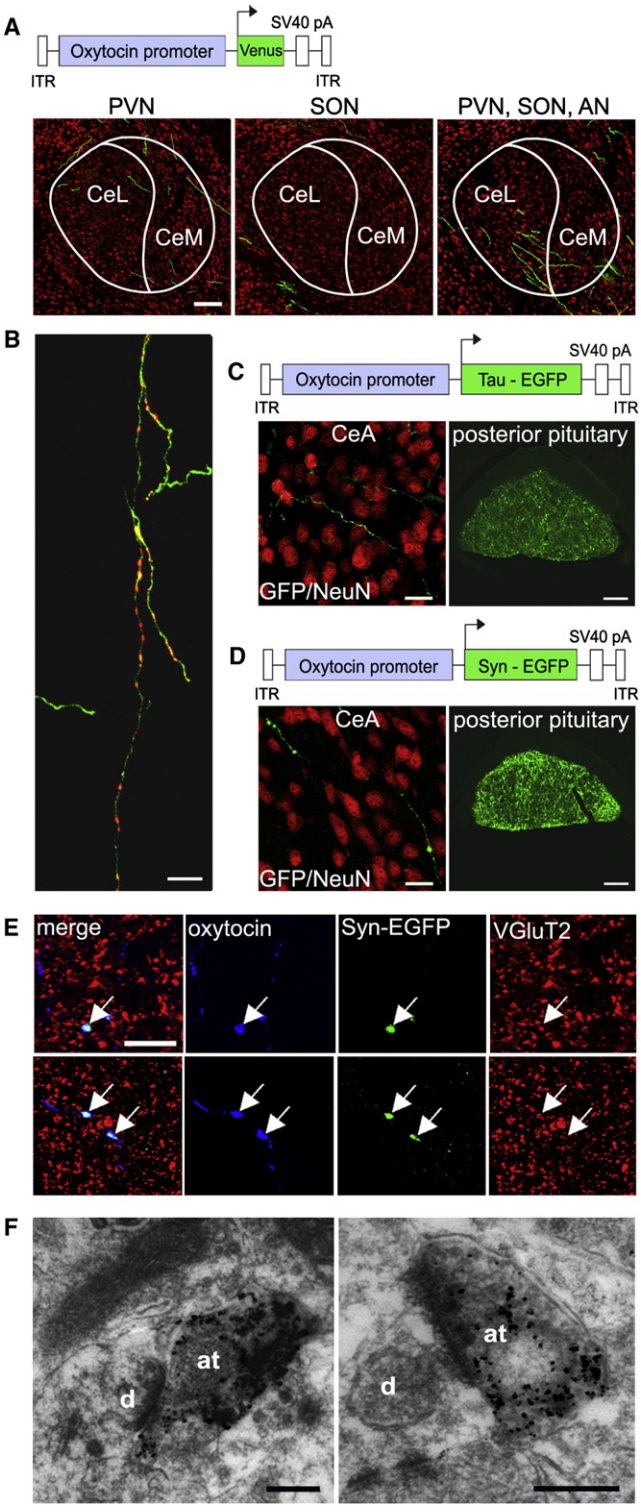

Figure 3. Venus-Positive Fibers from OT Neurons within the CeA Exhibit Axonal Features and Form Synapses

(A) Venus-positive fibers in the CeA originate from the PVN, SON, and AN and are infected with rAAV-expressing Venus from the OT promoter. The confocal images of the right CeAs were taken from coronal sections of the nucleus at Bregma, −2.7 mm. The external borders and the approximate borders between CeL (comprising two parts, the central central and central lateral) and the CeM are outlined.

(B) OT-immunoreactive puncta along Venus-positive fibers.

(C and D) Tau-EGFP (C) and Synaptophysin-EGFP (D) signals detected in OT fibers within the CeA and posterior pituitary. In (A)–(D), the brain sections were costained with antibody against the neuronal marker NeuN and were visualized in red by CY-3 conjugated antibodies.

(E) Synaptophysin-EGFP puncta overlap with OT and VGlut2.

(F) Asymmetric synapses in the CeL, formed by GFP-positive axonal terminals (at) of OT neurons on dendrites (d) of amygdala neurons. Scale bars represent 100 μm in (A), 5 μm in (B) and (E), 10 μm in left panels in (C) and (D), 100 μm in right panels in (C) and (D), and 250 nm and 500 nm for left and right electronograms, respectively, in (F).

Having shown functional ChR2 expression in the OT cell bodies, we tested whether BL could also release endogenous OT from axonal projections in horizontal slices of the CeA (Figure 4B, bottom). Exposure of the CeL to BL (20 s) evoked clear, reversible increases in AP frequencies in one-third (11/33) of CeL neurons in cell-attached recordings (from 0.24 ± 0.02 to 0.85 ± 0.24 Hz; Student's t test, $p < 0.01$; Figures 4D1 and 4D2). Preincubation with the OT-receptor antagonist (OTA), though not affecting basic AP frequencies, significantly and reversibly blocked these increases (>70% remaining response 0.46 ± 0.09 Hz, n = 5; one-way analysis of variance [ANOVA], $p < 0.05$; Figures 4D1 and 4D2). The GABA(A) blocker picrotoxin (PTX) caused, on average, a significant increase in baseline AP frequencies (from 0.27 ± 0.09 to 0.61 ± 0.26 Hz, n = 5; one-way ANOVA, $p < 0.05$), possibly as a result of inhibition of local inhibitory circuits in the CeL (Ciocchi et al., 2010; Haubensak et al., 2010). In summary, endogenous release of OT from hypothalamic fibers leads to an efficient, OT-R-mediated activation of CeL neurons.

Because CeL neurons project to and release GABA in the CeM (Huber et al., 2005), we also tested for rapid transient increases in IPSC frequencies in the CeM. CeL exposure to BL (20 s) evoked abrupt increases in IPSC frequencies in 36 out of 107 tested CeM neurons (Figure 4B, bottom trace and Figure 4E1), on average from 0.5 ± 0.1 Hz to 3.7 ± 0.8 Hz (Figure 4E2, first panel; Student's t test, $p < 0.01$), without affecting average IPSC amplitudes (Figure S4B). These increases depended on the precise area exposed to BL. Thus, BL applied outside the CeL, e.g., focused on the CeM (Figure 4E2, fifth panel, n = 6), never modified IPSC frequencies in CeM neurons that responded with increases in IPSCs after BL exposure of the CeL. Similar to the AP increases in the CeL (Figure 4D2), these increases in IPSC frequencies in CeM were significantly and reversibly blocked by OTA (>70%, 1.3 ± 0.2 Hz, n = 9; one-way ANOVA, $p < 0.05$; Figure 4E2, third panel). Subsequent PTX application blocked spontaneous IPSCs as well as any further BL effects (n = 5, Figure 4E2, fourth panel), confirming the GABAergic nature of the observed responses.

Although OTA significantly inhibited BL-induced increases of AP frequencies in the CeL and IPSC frequencies in the CeM, in both cases small but significant responses remained. In both CeA subdivisions, these responses could be entirely abolished by adding the AMPA-receptor antagonist NBQX to the OTA incubations (Figure 4D2, left panel, 0.25 ± 0.01 Hz for APs, n = 5; and Figure 4E2, third panel, 0.6 ± 0.1Hz for IPSCs, n = 4). This

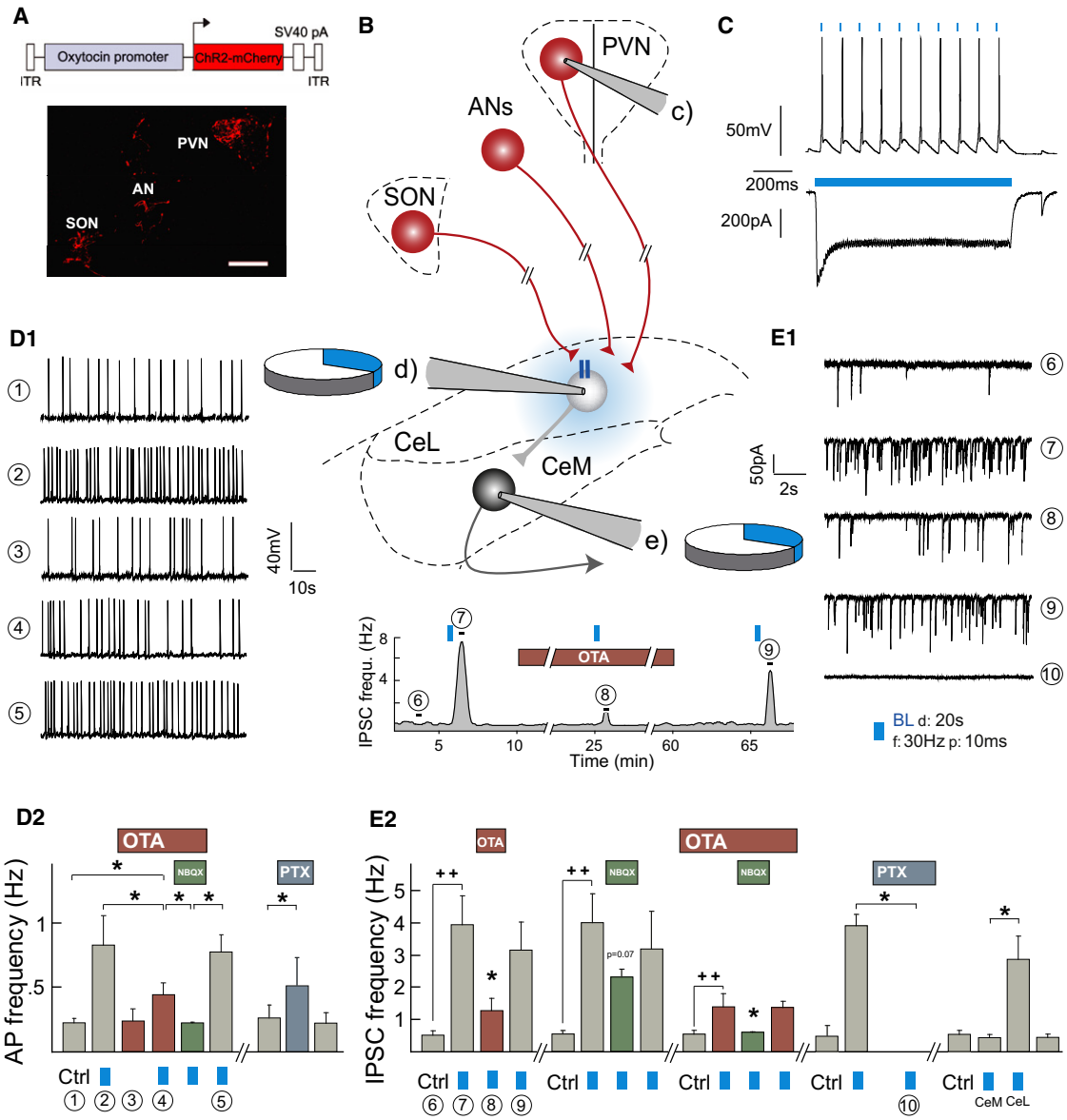

Figure 4. ChR2-Evoked Oxytocin Release from Fibers in the CeA

(A) The PVN, SON, and AN (coronal section) display mCherry expression after infection with OT promoter-ChR2-mCherry rAAV.

(B) Scheme of experimental set up showing (in coronal plane) the three hypothalamic nuclei and (in horizontal plane) the electrophysiological slice preparation (see Experimental Procedures). Labels c, d, and e refer to pipettes used for recordings in (C), (D1) and (D2), and (E1) and (E2), respectively, with pie charts indicating proportions of cells responding to BL.

(C) Action potentials evoked by 10 ms, 10 Hz, and currents induced by 1 s continuous BL stimulations in a fluorescent PVN cell.

(D1 and D2) Effects of 20 s BL (30 Hz, 10ms pulses) on CeL AP frequencies, both in CeL.

(D1) Example traces of APs recorded (1) without BL, (2) after BL, (3) with OTA alone, (4) with OTA + BL, and (5) BL after OTA washout.

(D2) Left: average AP frequencies of CeL neurons (1) without BL, (2) after BL, (3) with OTA alone, (4) OTA + BL, or (5) together with NBQX (n = 5) and after washout. Right: in presence of PTX without BL (n = 5).

(E1 and E2) Effects of BL in CeL (except where indicated) on IPSCs recorded in CeM neurons.

(E1) Example traces of IPSCs recorded (6) without BL, (7) after BL, (8) OTA + BL, (9) BL after OTA washout, and (10) BL in presence of PTX. (Example trace, below [B].) Rate-meter trace of IPSC frequencies recorded from a CeM neuron in response to (7) BL, (8) presence of OTA + BL, and (9) OTA washout + BL.

(E2) Average IPSC frequencies after BL in presence of OTA (first panel) (n = 9), NBQX only (second panel) (n = 5), both OTA and NBQX (third panel) (n = 4), PTX (fourth panel) (n = 4), and BL focused either on CeM or CeL (fifth panel) (n = 6). Statistical significances: Student's t test, ++ $p < 0.01$; one-way ANOVA, *$p < 0.05$. Blue squares represent BL stimulation.

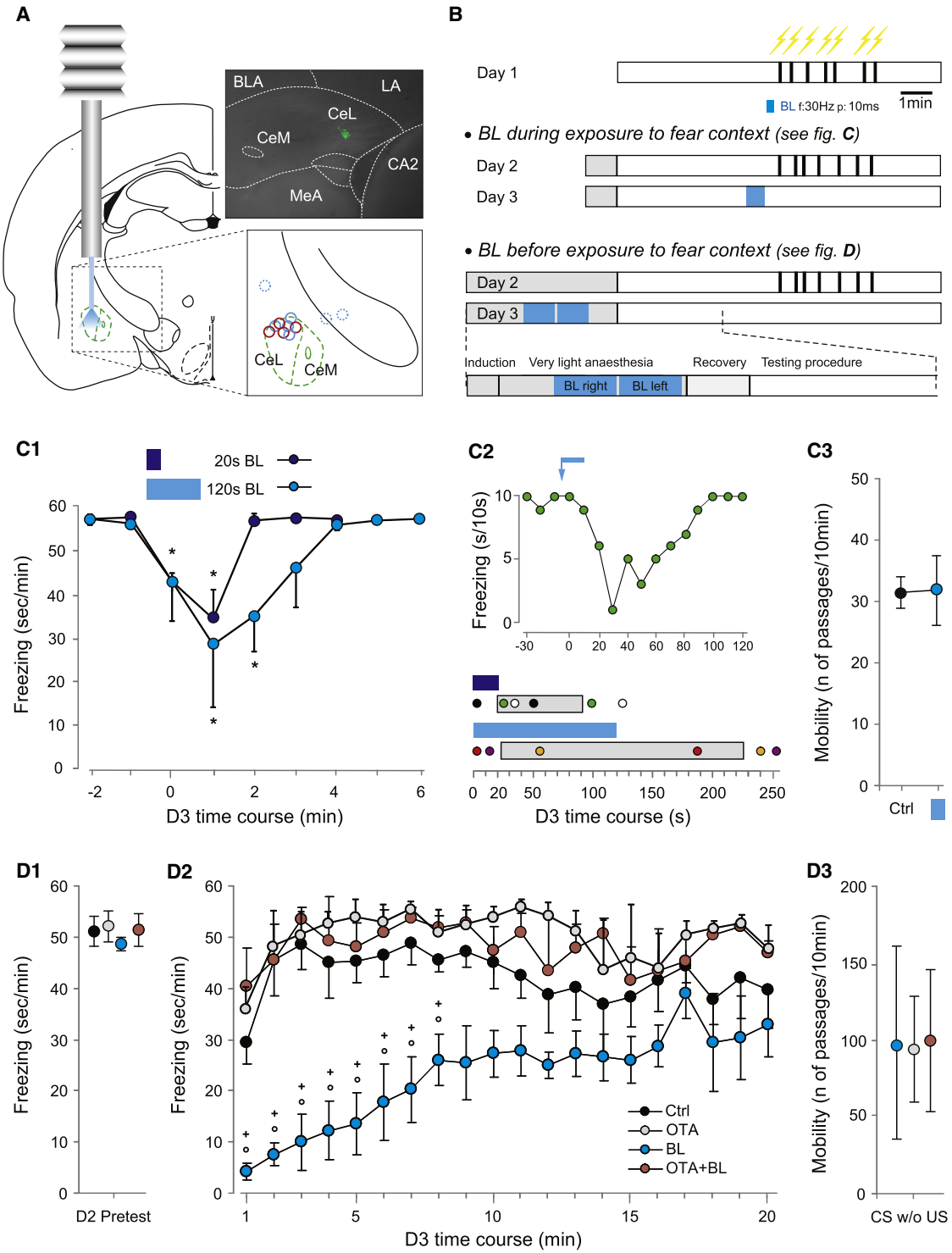

Figure 5. Evoked Release of Endogenous Oxytocin Attenuates Freezing Behavior

(A) Left: scheme of the placement of guide cannulae and optic fibers for BL application in CeL. Right: detail of the tip of the glass fiber position obtained after microinjection of fluorescent beads (see Experimental Procedures). Top right: example picture of fluorescent beads injected in CeL. Bottom right: example of eight correctly targeted CeLs in the left hemisphere (four of BL group, in blue; four of OTA + BL group, in red) and the three outliers (dotted blue circles).

(B) Three-day experimental contextual fear-conditioning protocol. Vertical black bars show the timing of foot shock during conditioning. Grey segments, pre-conditioning procedure including light anesthesia of the animal; blue segments, BL application.

(C1–C3) Effects of BL application during exposure to fear context.

suggests that the BL-evoked release of OT in the CeA is accompanied by the release of another factor, which requires AMPA-receptor activation. Indeed, we found that NBQX alone also decreased BL-induced IPSC responses in the CeM (Figure 4E2, second panel).

Blue-Light-Induced Activation of ChR2-Expressing OT Axons in the CeA Suppresses Contextual Freezing in Fear-Conditioned Rats

To determine whether BL-evoked release in vivo of endogenous OT in the CeA affects behavior, we expressed the ChR2-mCherry fusion protein in all hypothalamic OT structures of virgin female rats (see above). These rats were implanted bilaterally with guide cannulae to target blue-laser-coupled optical fibers above the CeA. Correct placement of the cannulae and fibers was verified by injections of fluorescent beads and post hoc analysis. Based on incorrect positioning, three rats (in which BL, as a consequence, did not decrease freezing responses) were excluded from further analysis. (Figure 5A, see also Experimental Procedures). To ensure basic activation of the amygdala during the behavioral experiments, we trained all rats in a 2-day contextual fear-conditioning protocol (see Figure 5B and Experimental Procedures) that resulted in similar freezing in the majority of animals (n = 25) after 2 days of conditioning (Figures 5C1 and 5D1). One animal was excluded from the experiment due to unusually low freezing levels. Hormonal cycle did not appear to affect these freezing levels (Figure S5).

To assess acute effects of BL on freezing behavior, we placed rats on day 3 in the fear-conditioning box after optic fibers had been inserted through the guide cannulae to target the CeL. All rats exhibited maximal freezing upon and throughout exposure to the context (Figure 5C1). After 10 min, 10 ms, 30 Hz BL pulses were given for either 20 or 120 s. As expected from the central role of the CeM in freezing behavior (Ciocchi et al., 2010; Haubensak et al., 2010) and the inhibitory effects of BL on the CeM in vitro (Figure 4), BL efficiently decreased freezing (from 57.5 ± 0.9 to 32.1 ± 5.6 s/min, n = 6; one-way ANOVA, $p < 0.05$; Figure 5C1). The onset of this decrease (Figure 5C2; see also Movie S1) started in two rats as fast as 2 s after BL onset and on average with a delay time of 21.5 ± 9.7 s across all animals (n = 6). Freezing returned after 70 ± 21 s upon termination of the 20 s BL stimulation and 108 ± 20 s after the 120 s BL exposure (n = 3 per group). The inhibiting effects of BL appeared specific to the fear-induced freezing response, because BL exposure in the same animals in a non-fear-conditioning context did not affect basic locomotor activity (Figure 5C3).

To confirm involvement of endogenous OT release in these BL responses, we injected OTA on day 3 through the same guide cannulae through which the optic fibers were subsequently inserted and applied BL immediately for 120 s before the rats were re-exposed (after removal of the optic fibers) to the fear-conditioning context. We thus measured the remaining block on the effects of BL by OTA, while at the same time providing more freedom of movement to the rats (now unobstructed by any attached optic fibers). We compared freezing behavior between four groups of rats, namely "Ctrl" (no BL, but optic fibers inserted prior to testing), "OTA" (OTA injected + optic fibers without BL), "BL" (BL application prior to exposure to context) and "OTA + BL" (injection of OTA followed by BL application prior to exposure to context). Ctrl or OTA-injected rats exhibited high freezing levels (Figure 5D2) comparable to those measured previously (Figure 5C1). On the other hand, BL-exposed rats immediately exhibited lower freezing levels upon exposure to the context. This reduced freezing persisted in these more freely moving rats over the first half of the testing period (Figure 5D2).

Of interest and importance, the BL inhibition of freezing was completely abolished in rats injected with OTA, which now exhibited similar freezing levels as rats that had not been exposed to BL (Figure 5D2). Because all rats demonstrated similar levels of freezing responses after 2 days of fear conditioning (Figure 5D1), and their mobility (tested by placing the animal in a different context) was not affected by BL exposure (Figure 5D3), these effects seem specific to the pharmacological and optogenetic exposures of the CeL. In conclusion, our in vivo findings, in addition to our in vitro findings, reveal that the activation of local OT fibers of hypothalamic origin triggers specific, OT-R-mediated reduction of fear responses, thereby further demonstrating the functional and physiological role of these OT projections.

Synaptic Contacts by Hypothalamic OT Projections as Revealed by Retrograde Tracing with Deletion-Mutant Pseudotyped Rabies Virus

The above findings suggest a specific targeting of OT from the hypothalamus to the CeA through local release from axonal endings. To retrogradely trace their precise cellular origins, we employed the deletion-mutant pseudotyped rabies virus SADΔG-EGFP (EnvA) (henceforth termed PS-Rab-EGFP, see Figure S6A for expression efficiency). We delivered into several hypothalamic projection sites, including the CeA, of 10-day pregnant rats (Figure 6A) two rAAVs expressing from the chicken β-actin-enhanced CMV promoter the avian sarcoma and leucosis virus receptor (TVA, coupled by IRES to tdTomato) and the rabies glycoprotein (RG). Expression of TVA is essential for PS-Rab entry into neurons, whereas expression of RG allows

(C1) Mean effects upon BL for 20 s (dark blue, n = 3) or 120 s (light blue, n = 3).
(C2) Top: example of BL effects on one animal. Each point represents the time of freezing during 10 s. Bottom: offset and return of total freezing for individual animals (color coded by dots) after 20 s (dark blue bar) or 120 s (light blue bar), with averages of dot values represented by gray bars.
(C3) Effect of BL on mobility, measured for the same animals, at day 4 in a different contextual box.
(D1–D3) Effects of BL application prior to exposure to the context.
(D1) Pretest quantification of freezing behavior obtained at the end of conditioning day 2.
(D2) Time course of freezing behavior for control (Ctrl, n = 4), 120 s BL (BL, 30Hz, 10ms pulses, n = 4), after OTA + BL (OTA + BL, n = 4), and after OTA alone (OTA, n = 4).
(D3) Mobility of different groups of animals (OTA, BL, and OTA + BL) at day 3 in the context without exposure to US during day 1 and 2 (n = 3 per group). Statistical significance: one-way ANOVA,*$p < 0.05$ in (C1)–(C3); two-ways ANOVA, + $p < 0.05$ BL versus Ctrl; $p < 0.05$ BL versus OTA + BL in (D1)–(D3).

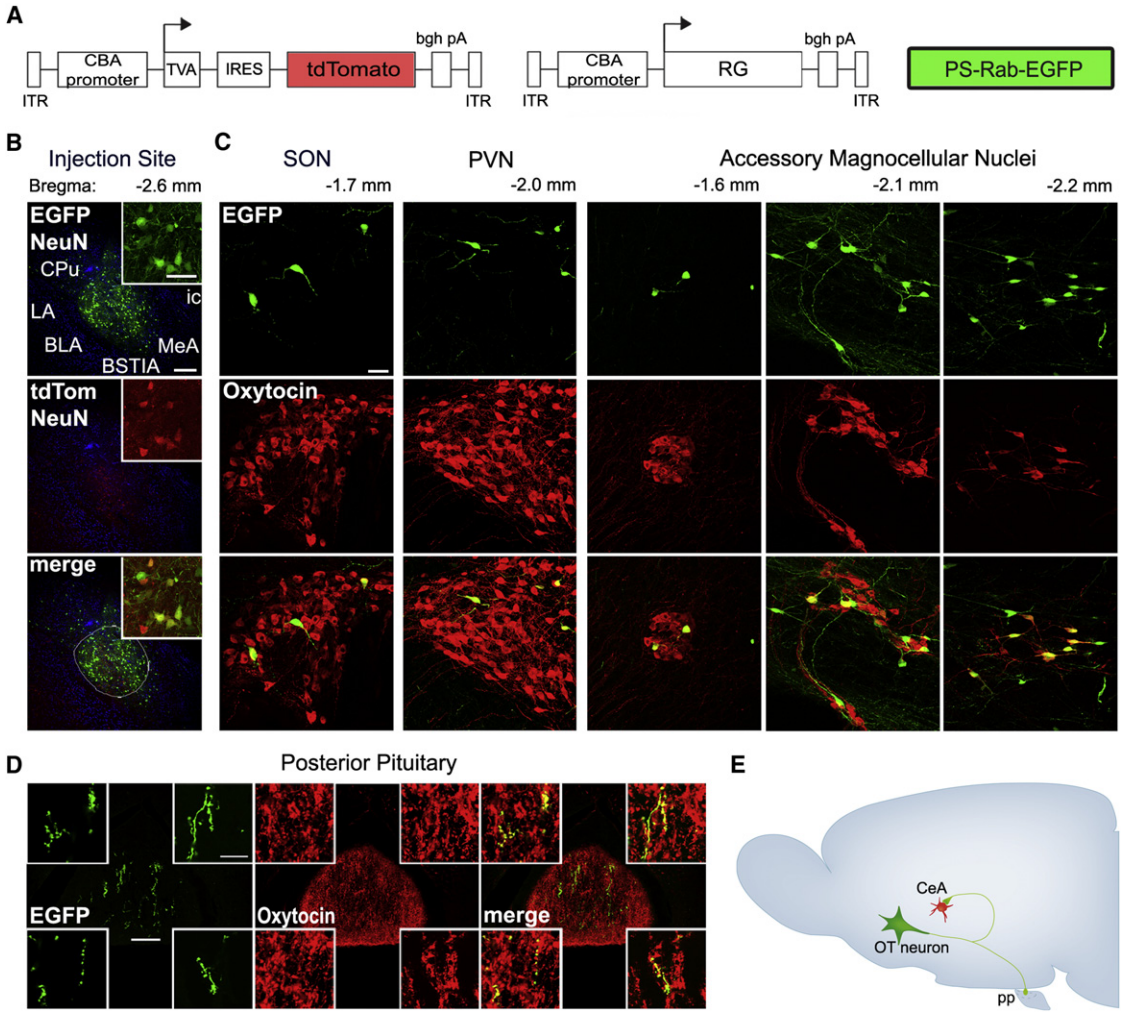

Figure 6. PS-Rab-Based Retrograde Labeling of Hypothalamic OT Neurons Monosynaptically Projecting to the CeA

(A) Pregnant rats were injected into the CeA with rAAVs expressing TVA-IRES-tdTomato and RG, followed by PS-Rab-EGFP.

(B) Primary infected neurons in the CeA show colocalization of tdTomato and EGFP (insets).

(C) Retrogradely labeled OT-positive neurons found in the SON, PVN, and especially in AN.

(D) EGFP-positive axonal endings in the posterior pituitary are also positive for OT (insets), indicating that magnocellular OT neurons project axons to the posterior pituitary and CeA.

(E) Schematic drawing of results in (C) and (D). Green cell denotes OT neurons, which project green collaterals simultaneously to the central sites (CeA, red cell) and to the posterior pituitary, from where OT reaches general circulation. Scale bars represent 100 μm in (B) and (D), 20 μm in the inset of (B), 50 μm in (C), and 20 μm in the insets of (D). BLA, basolateral amygdala; BSTIA, bed nucleus of stria terminalis (intraamygdaloid division); CPu, caudate putamen; ic, internal capsule; LA and MeA, lateral and medial amygdala; pp, posterior pituitary.

monosynaptically restricted retrograde transsynaptic transmission of PS-Rab (Wickersham et al., 2007). Subsequent injection of PS-Rab-EGFP into the same sites (CeA; Figure 6A) permitted analysis of retrogradely connected neurons on day 7 of lactation. Whereas primarily infected neurons in the injected sites should emit both red (tdTomato) and green (EGFP) fluorescence, retrogradely labeled neurons should emit green fluorescence only (Figure 6B). After infection of the CeA, we found EGFP-positive neurons mostly in the areas surrounding the PVN and SON, with a small number of neurons containing both OT and EGFP immunoreactivity (Figure 6C). As expected from the anterograde-labeling study (see Figure 3A), the highest number of double-positive neurons was observed within the AN (Figure 6C), identifying the AN as the major source for the OT innervation of the CeA. Neurons expressing only green fluorescence were also observed in various extrahypothalamic sources of CeA innervation (Figure S6B; Swanson and Petrovich, 1998), and injections of both rAAVs in two other hypothalamic targets (the nucleus accumbens, Acb, and nucleus of solitary tract, NTS) also resulted in EGFP-positive neurons in the hypothalamus (Figure S6C), attesting to the efficient retrograde monotranssynaptic labeling with this method. Thus, these findings confirm the presence of functional monosynaptic hypothalamic projections in the CeA.

Magnocellular OT Neurons Control CeA-Dependent Fear Responses

Hypothalamic nuclei contain magno- and parvocellular OT neurons, which are nonsegregated within the PVN (Swanson and Sawchenko, 1983), and both were indeed labeled by our OT-specific rAAVs (see Figure 1B; Figure S1A). Because magnocellular neurons, in contrast to parvocellular neurons, also send collateral branches to the posterior pituitary in addition to the extrahypothalamic forebrain, retrograde labeling of magnocellular brain projections may anterogradely label posterior pituitary endings. We used pseudotyped rabies virus to identify the magno- versus parvocellular origin of forebrain projections. Infection of CeA and Acb by PS-Rab-EGFP resulted in a fluorescent label in the pituitary in both cases (Figures 6D and S6C, top), but not following infection of the NTS (Figure S6C, bottom panel). Injection of the unpseudotyped rabies virus (UPS-Rab) in the pituitary (which can infect intact or damaged axons without the presence of TVA receptor) did not lead to labeling in the hypothalamus (Figure S6D), thereby confirming the specific transsynaptic labeling by PS-Rab. In summary, although these findings do not exclude a contribution by the parvocellular OT neuron population to innervation of all three nuclei, they provide clear evidence for the magnocellular origin and axon collateral nature of OT fibers in the CeA and Acb.

DISCUSSION

A longstanding unresolved question in the field of OT signaling in the brain concerns the precise sites of OT release and the pathways and mechanism through which OT reaches its target structures. The prevailing hypothesis in the field has been in favor of a dendritic release of OT in the hypothalamus, followed by OT diffusion to target areas. Through a combination of anatomical, electrophysiological, optical, and behavioral approaches, we provide in the present study morphological and functional evidence for the presence of axonal endings through which OT, produced in the hypothalamus, can reach the CeA and be locally delivered to exert direct effects both at the cellular and behavioral level.

Magnocellular OT Neurons Project Axonal Collaterals to Diverse Brain Regions

Application of cell-type-specific rAAV results in infection of the vast majority of OT neurons in both virgin and lactating rats. However, taking advantage of the higher transcriptional activity of virally introduced OT promoter in lactating rats and, hence, higher levels of expression of Venus (at least 3-fold; Figures 1C and S1) we visualized and semiquantified OT projections in 34 forebrain regions. The distribution of Venus-positive fibers in the forebrain agreed with anatomical studies from the 1980s (Sofroniew, 1983; Buijs, 1983), which showed OT-immunoreactive fibers in a limited number of forebrain structures, such as the tenia tecta, Acb, lateral septum, amygdala, and hippocampus. However, due to our highly sensitive method for detecting soluble marker proteins (Grinevich et al., 2005) and higher levels of Venus expression in lactating rats, we found many more fine Venus-positive axons in all major forebrain regions than by direct staining for OT. Moreover, classical immunohistochemistry does not reveal the sources of these fibers, which may originate from the PVN, SON, or AN. According to our results, the PVN and AN neurons project extensively to forebrain structures, whereas the SON contributes less to forebrain innervation. But even from the SON, which features only magnocellular neurons, a moderate number of fibers were observed in five forebrain regions (the horizontal limb of the diagonal band of Broca, Acb, CeA, lateral septum, and CA1 of the ventral hippocampus).

Additional evidence that magnocellular neurons project to higher brain regions was obtained with PS-Rab delivered into the CeA or the Acb. After injection of EGFP-expressing PS-Rab into these structures, we observed EGFP-positive back-labeled OT neurons residing in magnocellular nuclei, as well as their axonal terminals in the posterior pituitary. Importantly, only magnocellular hypothalamic neurons, but no other neuronal cell types, project to the posterior pituitary lobe (Brownstein et al., 1980; Sofroniew, 1983; Swanson and Sawchenko, 1983; Burbach et al., 2001).

In support of our observations, injection of the retrograde marker fluorogold into the Acb of voles led to the appearance of back-labeled OT neurons in the PVN and SON, with fluorogold-containing terminals in the posterior pituitary (Ross et al., 2009). In contrast, injection of PS-Rab into the NTS (Figure S6B) resulted in back-labeling of PVN parvocellular OT neurons, which do not project to the posterior pituitary (Sawchenko and Swanson, 1983; Swanson and Sawchenko, 1983). Collectively, the PS-Rab data in conjunction with light and, in particular, electron microscopic results provide compelling evidence that the fibers in the CeA and Acb are axonal collaterals of magnocellular OT neurons.

Our finding that magnocellular OT neurons simultaneously project to forebrain structures and the posterior pituitary is consistent with results demonstrating that the induced central and peripheral OT releases can be associated, for instance, in a situation of stress (Neumann, 2007). More specifically, it was previously demonstrated that an ethologically relevant stressor (such as forced swim in rats) induces an increase in OT plasma levels (Wotjak et al., 1998), as well as OT release within the CeA.

Inhibitory Effects of Endogenous OT Release in the Central Amygdala

Our anatomical results provide the basis for OT action within the CeA in both virgin and lactating rats. Although the density of OT fibers is lower in virgin than in lactating animals, the profile of axonal innervation of the CeA was similar in animals of both groups. In the CeM, we detected smooth nonbranching fibers which exceed the axons in the CeL in length. This type of fiber appears to represent transitory axons, traversing the CeM with no synaptic contacts. The appearance of axons in the CeL was strictly different: they exhibited single small branches, often possessing varicosities (as a substrate for presynaptic terminals; see Figures 3F, S3A, and 6), which may also represent sites for axonal OT release.

In accordance with this proposition, we found that release of endogenous OT from axonal endings, triggered by blue-light exposure of the CeL (but not the CeM), significantly modified the CeA signaling by increased activity of GABAergic interneurons in the CeL through an OT-R-dependent process. The

activation of these CeL neurons caused an increase of postsynaptic currents in CeM neurons, which were completely abolished by GABA(A) receptor antagonists, thus identifying their inhibitory nature. Accordingly, this increase of endogenous OT, by inhibiting neurons in the CeM, the main output center of the CeA, caused an attenuation of the freezing response (see below). It therefore appears that even relatively sparse innervation by OT-releasing axons in the CeL is sufficient to trigger significant inhibition through activation of GABAergic neurons projecting from the CeL to the CeM.

Our light and electron microscopic results demonstrate that OT neurons form synapses in the CeL analogous to OT-containing synapses within the SON (Theodosis, 1985), NTS (Peters et al., 2008), and at the lateral border of the hypothalamic ventromedial nucleus (Griffin et al., 2010). Furthermore, the asymmetric nature of these synapses and the occurrence of VGluT2 in the OT axons raise the question whether glutamate may be coreleased with OT. Both our recordings in the CeL and CeM indeed revealed, in the presence of the OT-R antagonist OTA, a remaining blue-light-evoked response that could be efficiently blocked by AMPA-receptor blockade, consistent with presynaptic glutamate release. Only application of NBQX revealed that AMPA-receptor activation is not required for OT release, which would preclude an involvement of presynaptic AMPA receptors on OT fibers. However, other ionotropic and possibly metabotropic glutamate receptors may facilitate OT release by contributing to axonal depolarization upon presynaptic glutamate release. In view of the recent discovery of distinct, mutually inhibitory neuronal populations in the CeL (Ciocchi et al., 2010; Haubensak et al., 2010), it will be of interest to determine how individual neuronal activity in this nucleus may be differentially affected by endogenous OT and/or glutamate release.

Behavioral Effects of Endogenous OT Release in Amygdala

A considerable and long-standing body of evidence indicates that OT can exert important effects on anxiety and fear responses by its effects in the CeA, following initial studies by Roozendaal and coauthors (Roozendaal et al., 1992a, 1992b, 1993). Further, in vivo experiments indicated that enhanced hypothalamic OT expression (Caldwell et al., 1987) and dendritic release (Neumann, 2007) might underlie the alterations in behavioral patterns seen during lactation, such as anxiety and aggression (Ferris et al., 1992; Lubin et al., 2003). Notably, in a rat strain with high anxiety-related behavior, the CeA level of OT was prominently increased in parallel with more intense maternal care, maternal offensive, and stress-coping behaviors, and these effects were reversed by local OTA infusion (Bosch et al., 2005). Very recent work also reports an effect on fear behavior by exogenous OT infusion into the CeA (Viviani et al., 2011). In this context, our study demonstrates that the blue-light-stimulated release of endogenous OT in the CeA drastically suppresses freezing behavior of fear-conditioned rats, with the effect abolished by infusion of OTA. The rapid onset and the time course of the reversibility of these effects provide further evidence in favor of a local release of OT from these fibers in the central amygdala, as opposed to slow diffusion from distant hypothalamic nuclei.

Our retrograde transsynaptic tracing with PS-Rab further assigned a magnocellular origin for OT in the hypothalamus. Indeed, Krause et al. (2011) reported recently how an osmotic challenge (dehydration) specifically activated OT-producing magnocellular neurons in the PVN, which in turn evoked profound anxiolytic effects. Taken together, these findings place the magnocellular neurons at a crucial intersection of transmitting environmental stimuli to the amygdala and provide a pathway through which these stimuli can lead to rapid OT-mediated regulation of anxiety and fear responses.

In conclusion, we employed an efficient and specific OT promoter, which allowed us to genetically manipulate OT neurons via insertion or deletion of genes of interest. Although we demonstrated the cell-type-specific targeting of OT neurons in rats and mice (unpublished data), the same OT promoter should work in other species because it is highly conserved among mammals. Furthermore, our evidence for functional OT axons in the CeA provides proof of principle for the local, targeted release of a modulatory neuropeptide by long-range axon collaterals in other forebrain regions, which can be used to specifically control region-associated behaviors. Our physiological and anatomical findings now open the technical prospect for studying the effects of endogenous OT release in various brain regions with respect to distinct forms of social behavior (Landgraf and Neumann, 2004; Ludwig and Leng, 2006; Donaldson and Young, 2008; Lee et al., 2009; Ross and Young, 2009). Because the role of OT in human psychopathology has become subject of many translational studies (De Dreu et al., 2010; Simeon et al., 2011; Skrundz et al., 2011), the experimental alteration in endogenous OT release may open the way to dissect OT-related pathogenic mechanisms underlying emotional and psychiatric disorders in human patients.

EXPERIMENTAL PROCEDURES

Cloning of rAAV Vectors

For generating rAAVs with specific expression in OT cells, we used the software BLAT from University of California, Santa Cruz (http://genome.ucsc.edu/cgi-bin/hgBlat) and selected a conserved 2.6 kb promoter directly upstream of the OT gene exon 1. This DNA was amplified from an EcoRI-linearized BAC clone RP24-388N9 (RPCI-24 Mouse, BACPAC Resources) using a 5′ primer containing a NotI-restriction site (5′-ATTAGCGGCCGCA GATGAGCTGGTGAGCATGTGAAGACATGC-3′) and a 3′ primer with a SalI-restriction site (5′-ATTAGTCGACGGCGATGGTGCTCAGTCTGAGATCCGCT GT-3′), subcloned into pBlueScript SK and further cloned into the rAAV2 backbone, pAAV-αCaMKII-htTA, thereby substituting the αCaMKII-promoter. The resulting rAAV expression vector was used for exchange of the htTA-gene for the following genes of interest: Venus, Channelrhodopsin-2 -mCherry, Tau-EGFP, and Synaptophysin-EGFP.

We also designed rAAV vectors equipped with the cytomegalovirus enhancer/chicken-β-actin promoter, expressing the rabies glycoprotein (RG) and the avian sarcoma and leucosis virus (TVA) receptor linked via an internal ribosomal entry site (IRES) to the fluorescent marker tdTomato.

Production of rAAVs

Production and purification of rAAVs (Serotype 1/2) were as described (Pilpel et al., 2009). rAAV genomic titers were determined with QuickTiter AAV Quantitation Kit (Cell Biolabs) and RT-PCR using the ABI 7700 cycler (Applied Biosystems). rAAVs titers were $\sim 10^{10}$ genomic copies per μl.

Rabies Viruses

Propagation of PS-Rab was performed as reported previously (Wickersham et al., 2010; Rancz et al., 2011). Briefly, after infection of BHK-B19G cells by SADΔG-GFP or SADΔG-mCherry, the supernatant containing unpseudotyped deletion-mutant rabies virus (UPS-Rab) was filtered and stored at −80°C (Figures S6A and S6D). Rabies virus pseudotyping (Wickersham et al., 2010; Rancz et al., 2011) and purification were as with lentivirus (Dittgen et al., 2004).

Animals

For anatomical studies, adult female Wistar rats were separated into 11 groups, according to the purposes of the study (Table S1). For stereotactic coordinates (Paxinos and Watson, 1998) and volumes of virus-containing solution, see Table S2. Stereotactic injections were performed as described (Cetin et al., 2006).

Histology

Double Fluorescence Immunohistochemistry

Vibratome sections of brains (50 μm) perfused with 4% paraformaldehyde (PFA) were stained with chicken anti-GFP (Abcam; 1:10,000) and combined with various antibodies against the following: OT and VP (1:300; provided by Harold Gainer; Ben-Barak et al., 1985); NeuN (Chemicon; 1:1,000); VGluT2 (Synaptic Systems; 1:1,000); and tdTomato (1:1,000; Clonthech). Whereas Venus and EGFP signals were enhanced by FITC-conjugated IgGs, other proteins and markers were visualized by CY3-conjugated or CY5-conjugated antibodies (1:300; Jackson Immuno-Research Laboratories). All images were acquired on a confocal Leica TCS NT and Zeiss LSM5 microscopes; digitized images were analyzed using Adobe Photoshop (Adobe).

Cell-Type Specificity and Inducibility of Venus Expression in OT Neurons

To analyze the specificity of OT promoter-Venus rAAV in neurons of the PVN and SON, we counted all Venus- and OT-immunoreactive neurons (80–150 neurons/section dependent on the anterior-posterior Bregma level) in three sections per animal at three different rostro-caudal Bregma levels (PVN: −1.5, −1.8, and −2.0 mm; SON: −1.1, −1.4, and −1.7 mm). Sections were taken from three virgin rats and three lactating rats, the latter killed on day 14 after parturition. For the analysis of the AN of three virgin and three lactating rats, we counted all Venus- and OT-immunoreactive neurons in two sections per animal (due to the shorter anterior-posterior extent of the AN compared to the SON and PVN) at two different Bregma levels (rSON: −2.0 and −2.1 mm; CN: −1.4 and −1.5 mm; DLN: −2.1 and −2.2 mm) and on average per section 12 neurons for the CN, 35 neurons for the DLN, and 19 neurons for the rSON. The number of identified and counted cells in both groups of animals was 4,774 neurons in total (more details on cell numbers are in Table 1). The comparison between the numbers of identified neurons per each rat and structure between groups of virgin and lactating rats was evaluated statistically (see below). The duration of infection was similar in all animals (25 days; see Table S1).

To exclude the possibility that our viral vector also infects VP neurons, the same analysis was performed on SON sections of three rats (see above). The sections were costained with antibodies against OT (visualized by CY3-conjugated secondary antibodies) and VP (visualized with CY5-conjugated antibodies) for subsequent counting of all cells visible in the SON positive for Venus, OT, and VP at three different Bregma levels (−1.1, −1.4, and −1.7 mm).

To analyze the inducibility of our viral vector, we analyzed the SONs of pregnant rats and virgin rats 1 day before delivery, on the day of delivery, and the day after delivery with Fiji (National Institute of Mental Health) to manually measure direct fluorescence intensity and cell sizes (25 cells/section; 3–4 sections per rat, 3 rats in each group, 12 animals in total). The selection of cells in the SON was done randomly at similar Bregma levels of the rostro-caudal extend of the nucleus (Bregmas: −0.92, −1.3, −1.4, and −1.6 mm). The total number of cells counted in each group was 180 (virgins), 180 (day before delivery), 240 (day of delivery), and 180 (day after delivery).

Statistical significance was determined by Student's t test for colocalization experiments and by one-way ANOVA for the inducibility of virally introduced OT-promoter fragment during peripartum period. Statistical analysis was performed with use of Prism 5 for Mac OS X. Results are presented as mean ± SEM. $p < 0.05$ were considered statistically significant.

Electron Microscopy

Rats were perfused transcardially with 4% PFA in phosphate buffer containing 0.05% glutaraldehyde at pH 7. The 50 μm coronal brain sections containing the CeA were incubated with rabbit polyclonal anti-GFP antibodies (Molecular Probes; 1:5,000). The GFP signals were visualized using the standard avidin-biotin complex protocol and DAB chromogen, intensified by silver-gold (Liposits et al., 1986) and processed (Eliava et al., 2003).

Electrophysiological In Vitro Experiments

Slice Preparation. Four-to-eight weeks after injection of ChR2-mCherry rAAV into the SON, PVN, and AN of adult virgin female rats, brains were removed, cut into 400 μm horizontal slices (described in Huber et al., 2005), and kept in artificial cerebrospinal fluid in the dark to avoid ChR2 activation.

Electrophysiological Recordings. Whole-cell patch-clamp recordings were visually guided by infrared videomicroscopy (DM-LFS; Leica), using 4–9 MOhm borosilicate pipettes filled with 140 mM KCl, 10 mM HEPES, 2 mM $MgCl_2$, 0.1 mM $CaCl_2$, 0.1 mM BAPTA, 2 mM ATP Na salt, 0.3 mM GTP Na salt (pH 7.3), 300 mOsm, and amplified with an Axopatch 200B (Axon Instruments). For cell-attached recordings, KCl was replaced with KMeSO4. ChR2-mCherry expression was identified by fluorescent microscopy and post hoc immunohistochemistry.

Blue-Light Stimulation. For in vitro experiments, optical stimulation was done via a mercury lamp (Short Arc 103W/2, Osram; ∼5 mW/mm^2) in combination with a shutter (VS25S22M1R1, Uniblitz) or a TTL-pulsed LED source (LXHL-LB3C, Roithner; ∼10 mW/mm^2), both yielding similar results.

Behavioral Experiments

Fear Conditioning

Following recovery from guide cannulae implantation (1 week), female virgin rats of random hormonal cycle were exposed to a contextual fear-conditioning protocol. This consisted of three sessions on consecutive days (Figure 5B). On day 1, rats were individually introduced in the conditioning box (45 × 18 × 25 cm) and after 10 min received a first series of seven electric shocks (0.8 mA) at random intervals (15–120 s) over 7 min. After the last shock, the rats were left in the box for 3 more min. BL was applied in 10-ms pulses at 30 Hz via a glass fiber protruding 2 mm beyond the lower end of the cannulae and delivered light intensity of ∼10 mW. OTA injection was done via two injectors (cut to fit the 5.8 mm guide cannulae protruding 2 mm beyond the lower end of the cannulae) that were bilaterally lowered into the guide cannulae, connected via polyten tubing to two Hamilton syringes that were placed in an infusion pump, and 0.5 μl of liquid containing 21 ng OTA was injected in each hemisphere at 0.25 μl/min over a 2 min period.

Application of BL during Fear-Context Exposure. On day 2, the rats were habituated to the glass fibers by inserting them into the cannulae for the complete duration of the protocol, which was similar to the one of day 1 (Figure 5C). On day 3, the rats were tested in the context for 10 min before receiving bilateral BL stimulation for either 20 s or 120 s. The effect was video recorded for the complete 20 min of the test (see Figure 5B). Freezing time was analyzed per 10 s intervals.

Application of BL prior to Fear-Context Exposure. On day 2, rats received in addition a sham blue-light application during 6 min of very light isoflurane (5% induction, 1% for maintenance), during which time the glass fiber was inserted into the guide cannulae, as on day 3, without exposure to BL (Figure 5D). At the end of day 2, freezing levels were assessed to exclude differences possibly caused by the implantation of the cannulae before the rats were divided in four groups for testing on day 3 (see Figure 5D). On day 3, the rats received (1) sham BL (insertion of the glass fiber without exposure to BL), (2) BL, (3) OTA alone, or (4) OTA and BL. BL was applied bilaterally for 2 min, first on the right and then on the left hemisphere. Rats were allowed 2 min of recovery from anesthesia and introduced in the context, where their behavior was video recorded during a 20 min period without electric shocks. Freezing was assessed per periods of 1 min intervals.

Effects of BL on Mobility. Animal mobility was assessed using photobeam sensors placed at 1 cm distances. Each time of beam interruption by the rat was counted by the software as one passage (MED-PC, Med Associates).

Blue-Light Stimulation In Vivo and Verification of Optic Fiber Positions

For the in vivo experiments, we used two blue lasers (λ 473nm, output of 150 mW/mm^2, DreamLasers) coupled with optical fibers (BFL37-200-CUSTOM,

EndA = FC/PC, and EndB = FLAT CLEAVE; Thorlabs), which were directly inserted above the region of interest via guide cannulae (C313G-SPC 22 Gauge, 5.8 mm below pedestal, PlasticOne). Guide cannulae were chronically implanted under isoflurane anesthesia (5% induction, 2% maintenance) at stereotaxic positions of −2.5 mm anteroposterior and 3.9 mm lateral from Bregma and were stabilized with dental cement. On the days of the experiments, the optic fibers were inserted through the cannulae and fixed through a screw at a position 2 mm protruding beyond the lower end of the cannula. This should lead to a specific stimulation of the CeL, as prevalent measurements with BL stimulations in rodent brain have shown that the BL of the laser does not penetrate the tissue further than 500 μm (Yizhar et al., 2011).

After the behavioral experiments, 0.5 μl of green fluorescent latex microspheres (Lumafluor) was injected 2 mm below the lower end of the cannulae (i.e., the same position as the optical fibers). Rats were subsequently killed to assess the placement of the tip of the injector by sectioning the brain with a vibratome into 400 μm slices (see Figure 5A).

Drugs and Concentrations

Oxytocin-receptor antagonist d(CH2)5-Tyr(Me)-[Orn8]-vasotocin (1 μM, OTA, Bachem), glutamate-receptor (AMPA) antagonist 1,2,3,4-tetrahydro-6-nitro-2,3-dioxo-benzo[f]quinoxaline-7-sulfonamide (0.4 μM, NBQX, Sigma), (−) bicuculline methiodide (Sigma), or picrotoxin (50 μM, PTX, Sigma) were bath perfused for the in vitro experiments for 20 min before and several min beyond the expected response to BL application.

Data Acquisition and Analysis

Patch-clamp signals were acquired with pClamp 9.0 (Axon Instruments), filtered at 5 kHz, and digitized at 10 kHz with a Digidata 1200 A/D (Axon Instruments). Currents were detected and analyzed using Minianalysis Program 6.0 (Synaptosoft).

Statistical Analysis

Data in text are expressed as mean ± SEM.

For in vitro experiments, one-way ANOVA with factor treatment (i.e., respective drug used) was used for assessment of pharmacological effects; Student's t test was used for assessment of BL effect without drug.

For in vivo experiments, one-way ANOVA with factor time was used for assessment of the BL effect on both freezing and mobility; Student's t test was used for comparison of duration of BL effect. For the experiments in Figure 5D, two-way repeated ANOVA with factors treatment (Ctrl versus BL; Ctrl versus OTA + BL; BL versus OTA) and time were used for assessment of BL effect in presence of pharmacological effects on freezing response.

When the ANOVA test was significant, the Tukey test was used for post hoc multiple comparisons. Differences were considered significant for $p < 0.05$ (*, + and °; ANOVA) or $p < 0.01$ (++, t test). All statistical tests were performed with StatView 5 (StatView, SAS Institute).

SUPPLEMENTAL INFORMATION

Supplemental Information includes six figures, two tables, Supplemental Experimental Procedures, and one movie and can be found with this article online at doi:10.1016/j.neuron.2011.11.030.

ACKNOWLEDGMENTS

We thank Anna Illarionova and Natalie Landeck for the cloning of several viral vectors, Miriam Kernert for her help with injection of viruses into rat brains, Guenther Giese and Annemarie Scherbach for assistance with confocal microscopy, Sophie Koszinowski for help with experiments in peripartum rats, Rolf Sprengel for input into OT-promoter selection, Georg Koehr and Claudia Rauner for initial electrophysiological recordings, Edward Callaway and Karl K. Conzelmann for TVA and RG plasmids, Scott Sternson for the ChR2-mCherry rAAV vector, Matthias Klugmann for the GFAP-GFP rAAV vector, Daniel Huber, Marios Abatis, and Jérôme Wahis for advice or help with optogenetic experiments, Hannah Monyer for supporting the electron microscopic study, and Harold Gainer for antibodies against OT and VP. Supported by the Max Planck Society, grant SFB488 to P.H.S., grants GR 3619/2-1 and GR 3619/3-1 by the German Research Foundation to V.G., and the Chica and Heinz Schaller Research Foundation to V.G.

Accepted: November 28, 2011
Published: February 8, 2012

REFERENCES

Ben-Barak, Y., Russell, J.T., Whitnall, M.H., Ozato, K., and Gainer, H. (1985). Neurophysin in the hypothalamo-neurohypophysial system. I. Production and characterization of monoclonal antibodies. J. Neurosci. *5*, 81–97.

Bosch, O.J., Meddle, S.L., Beiderbeck, D.I., Douglas, A.J., and Neumann, I.D. (2005). Brain oxytocin correlates with maternal aggression: link to anxiety. J. Neurosci. *25*, 6807–6815.

Boyden, E.S., Zhang, F., Bamberg, E., Nagel, G., and Deisseroth, K. (2005). Millisecond-timescale, genetically targeted optical control of neural activity. Nat. Neurosci. *8*, 1263–1268.

Brownstein, M.J., Russell, J.T., and Gainer, H. (1980). Synthesis, transport, and release of posterior pituitary hormones. Science *207*, 373–378.

Buijs, R.M. (1983). Vasopressin and oxytocin—their role in neurotransmission. Pharmacol. Ther. *22*, 127–141.

Burbach, J.P.H., Luckman, S.M., Murphy, D., and Gainer, H. (2001). Gene regulation in the magnocellular hypothalamo-neurohypophysial system. Physiol. Rev. *81*, 1197–1267.

Caldwell, J.D., Greer, E.R., Johnson, M.F., Prange, A.J., Jr., and Pedersen, C.A. (1987). Oxytocin and vasopressin immunoreactivity in hypothalamic and extrahypothalamic sites in late pregnant and postpartum rats. Neuroendocrinology *46*, 39–47.

Cetin, A., Komai, S., Eliava, M., Seeburg, P.H., and Osten, P. (2006). Stereotaxic gene delivery in the rodent brain. Nat. Protoc. *1*, 3166–3173.

Ciocchi, S., Herry, C., Grenier, F., Wolff, S.B., Letzkus, J.J., Vlachos, I., Ehrlich, I., Sprengel, R., Deisseroth, K., Stadler, M.B., et al. (2010). Encoding of conditioned fear in central amygdala inhibitory circuits. Nature *468*, 277–282.

Davis, M. (2000). A functional analysis. In The Amygdala, J.P. Aggleton, ed. (New York: Oxford University Press), pp. 213–288.

De Dreu, C.K.W., Greer, L.L., Handgraaf, M.J.J., Shalvi, S., Van Kleef, G.A., Baas, M., Ten Velden, F.S., Van Dijk, E., and Feith, S.W.W. (2010). The neuropeptide oxytocin regulates parochial altruism in intergroup conflict among humans. Science *328*, 1408–1411.

Dittgen, T., Nimmerjahn, A., Komai, S., Licznerski, P., Waters, J., Margrie, T.W., Helmchen, F., Denk, W., Brecht, M., and Osten, P. (2004). Lentivirus-based genetic manipulations of cortical neurons and their optical and electrophysiological monitoring in vivo. Proc. Natl. Acad. Sci. USA *101*, 18206–18211.

Donaldson, Z.R., and Young, L.J. (2008). Oxytocin, vasopressin, and the neurogenetics of sociality. Science *322*, 900–904.

Eliava, M., Yilmazer-Hanke, D., and Asan, E. (2003). Interrelations between monoaminergic afferents and corticotropin-releasing factor-immunoreactive neurons in the rat central amygdaloid nucleus: ultrastructural evidence for dopaminergic control of amygdaloid stress systems. Histochem. Cell Biol. *120*, 183–197.

Ferris, C.F., Foote, K.B., Meltser, H.M., Plenby, M.G., Smith, K.L., and Insel, T.R. (1992). Oxytocin in the amygdala facilitates maternal aggression. Ann. N Y Acad. Sci. *652*, 456–457.

Gimpl, G., and Fahrenholz, F. (2001). The oxytocin receptor system: structure, function, and regulation. Physiol. Rev. *81*, 629–683.

Griffin, G.D., Ferri-Kolwicz, S.L., Reyes, B.A.S., Van Bockstaele, E.J., and Flanagan-Cato, L.M. (2010). Ovarian hormone-induced reorganization of oxytocin-labeled dendrites and synapses lateral to the hypothalamic ventromedial nucleus in female rats. J. Comp. Neurol. *518*, 4531–4545.

Grinevich, V., Brecht, M., and Osten, P. (2005). Monosynaptic pathway from rat vibrissa motor cortex to facial motor neurons revealed by lentivirus-based axonal tracing. J. Neurosci. *25*, 8250–8258.

Haubensak, W., Kunwar, P.S., Cai, H., Ciocchi, S., Wall, N.R., Ponnusamy, R., Biag, J., Dong, H.W., Deisseroth, K., Callaway, E.M., et al. (2010). Genetic dissection of an amygdala microcircuit that gates conditioned fear. Nature *468*, 270–276.

Hitchcock, J.M., and Davis, M. (1991). Efferent pathway of the amygdala involved in conditioned fear as measured with the fear-potentiated startle paradigm. Behav. Neurosci. *105*, 826–842.

Hökfelt, T. (1991). Neuropeptides in perspective: the last ten years. Neuron *7*, 867–879.

Huber, D., Veinante, P., and Stoop, R. (2005). Vasopressin and oxytocin excite distinct neuronal populations in the central amygdala. Science *308*, 245–248.

Kapp, B.S., Frysinger, R.C., Gallagher, M., and Haselton, J.R. (1979). Amygdala central nucleus lesions: effect on heart rate conditioning in the rabbit. Physiol. Behav. *23*, 1109–1117.

Kawasaki, A., Hoshi, K., Kawano, M., Nogami, H., Yoshikawa, H., and Hisano, S. (2005). Up-regulation of VGLUT2 expression in hypothalamic-neurohypophysial neurons of the rat following osmotic challenge. Eur. J. Neurosci. *22*, 672–680.

Krause, E.G., de Kloet, A.D., Flak, J.N., Smeltzer, M.D., Solomon, M.B., Evanson, N.K., Woods, S.C., Sakai, R.R., and Herman, J.P. (2011). Hydration state controls stress responsiveness and social behavior. J. Neurosci. *31*, 5470–5476.

Landgraf, R., and Neumann, I.D. (2004). Vasopressin and oxytocin release within the brain: a dynamic concept of multiple and variable modes of neuropeptide communication. Front. Neuroendocrinol. *25*, 150–176.

Lee, H.-J., Macbeth, A.H., Pagani, J.H., and Young, W.S., 3rd. (2009). Oxytocin: the great facilitator of life. Prog. Neurobiol. *88*, 127–151.

Liposits, Z., Sherman, D., Phelix, C., and Paull, W.K. (1986). A combined light and electron microscopic immunocytochemical method for the simultaneous localization of multiple tissue antigens. Tyrosine hydroxylase immunoreactive innervation of corticotropin releasing factor synthesizing neurons in the paraventricular nucleus of the rat. Histochemistry *85*, 95–106.

Lubin, D.A., Elliott, J.C., Black, M.C., and Johns, J.M. (2003). An oxytocin antagonist infused into the central nucleus of the amygdala increases maternal aggressive behavior. Behav. Neurosci. *117*, 195–201.

Ludwig, M., and Leng, G. (2006). Dendritic peptide release and peptide-dependent behaviours. Nat. Rev. Neurosci. *7*, 126–136.

McEwen, B.B. (2004). Brain-fluid barriers: relevance for theoretical controversies regarding vasopressin and oxytocin memory research. Adv. Pharmacol. *50*, 531–592, 655–708.

Meeker, R.B., Swanson, D.J., Greenwood, R.S., and Hayward, J.N. (1991). Ultrastructural distribution of glutamate immunoreactivity within neurosecretory endings and pituicytes of the rat neurohypophysis. Brain Res. *564*, 181–193.

Nagel, G., Szellas, T., Huhn, W., Kateriya, S., Adeishvili, N., Berthold, P., Ollig, D., Hegemann, P., and Bamberg, E. (2003). Channelrhodopsin-2, a directly light-gated cation-selective membrane channel. Proc. Natl. Acad. Sci. USA *100*, 13940–13945.

Navone, F., Di Gioia, G., Jahn, R., Browning, M., Greengard, P., and De Camilli, P. (1989). Microvesicles of the neurohypophysis are biochemically related to small synaptic vesicles of presynaptic nerve terminals. J. Cell Biol. *109*, 3425–3433.

Neumann, I.D. (2007). Stimuli and consequences of dendritic release of oxytocin within the brain. Biochem. Soc. Trans. *35*, 1252–1257.

Neumann, I.D. (2008). Brain oxytocin: a key regulator of emotional and social behaviours in both females and males. J. Neuroendocrinol. *20*, 858–865.

Paxinos, G., and Watson, C. (1998). The Rat Brain in Stereotaxic Coordinates, Fourth Edition (London: Academic Press).

Peters, J.H., McDougall, S.J., Kellett, D.O., Jordan, D., Llewellyn-Smith, I.J., and Andresen, M.C. (2008). Oxytocin enhances cranial visceral afferent synaptic transmission to the solitary tract nucleus. J. Neurosci. *28*, 11731–11740.

Pilpel, N., Landeck, N., Klugmann, M., Seeburg, P.H., and Schwarz, M.K. (2009). Rapid, reproducible transduction of select forebrain regions by targeted recombinant virus injection into the neonatal mouse brain. J. Neurosci. Methods *182*, 55–63.

Rancz, E.A., Franks, K.M., Schwarz, M.K., Pichler, B., Schaefer, A.T., and Margrie, T.W. (2011). Transfection via whole-cell recording in vivo: bridging single-cell physiology, genetics and connectomics. Nat. Neurosci. *14*, 527–532.

Roozendaal, B., Schoorlemmer, G.H., Wiersma, A., Sluyter, S., Driscoll, P., Koolhaas, J.M., and Bohus, B. (1992a). Opposite effects of central amygdaloid vasopressin and oxytocin on the regulation of conditioned stress responses in male rats. Ann. N Y Acad. Sci. *652*, 460–461.

Roozendaal, B., Wiersma, A., Driscoll, P., Koolhaas, J.M., and Bohus, B. (1992b). Vasopressinergic modulation of stress responses in the central amygdala of the Roman high-avoidance and low-avoidance rat. Brain Res. *596*, 35–40.

Roozendaal, B., Schoorlemmer, G.H., Koolhaas, J.M., and Bohus, B. (1993). Cardiac, neuroendocrine, and behavioral effects of central amygdaloid vasopressinergic and oxytocinergic mechanisms under stress-free conditions in rats. Brain Res. Bull. *32*, 573–579.

Ross, H.E., and Young, L.J. (2009). Oxytocin and the neural mechanisms regulating social cognition and affiliative behavior. Front. Neuroendocrinol. *30*, 534–547.

Ross, H.E., Cole, C.D., Smith, Y., Neumann, I.D., Landgraf, R., Murphy, A.Z., and Young, L.J. (2009). Characterization of the oxytocin system regulating affiliative behavior in female prairie voles. Neuroscience *162*, 892–903.

Sawchenko, P.E., and Swanson, L.W. (1983). The organization and biochemical specificity of afferent projections to the paraventricular and supraoptic nuclei. Prog. Brain Res. *60*, 19–29.

Simeon, D., Bartz, J., Hamilton, H., Crystal, S., Braun, A., Ketay, S., and Hollander, E. (2011). Oxytocin administration attenuates stress reactivity in borderline personality disorder: a pilot study. Psychoneuroendocrinology *36*, 1418–1421.

Skrundz, M., Bolten, M., Nast, I., Hellhammer, D.H., and Meinlschmidt, G. (2011). Plasma oxytocin concentration during pregnancy is associated with development of postpartum depression. Neuropsychopharmacology *36*, 1886–1893.

Sofroniew, M.V. (1983). Morphology of vasopressin and oxytocin neurones and their central and vascular projections. Prog. Brain Res. *60*, 101–114.

Swanson, L.W., and Petrovich, G.D. (1998). What is the amygdala? Trends Neurosci. *21*, 323–331.

Swanson, L.W., and Sawchenko, P.E. (1983). Hypothalamic integration: organization of the paraventricular and supraoptic nuclei. Annu. Rev. Neurosci. *6*, 269–324.

Theodosis, D.T. (1985). Oxytocin-immunoreactive terminals synapse on oxytocin neurones in the supraoptic nucleus. Nature *313*, 682–684.

Theodosis, D.T. (2002). Oxytocin-secreting neurons: A physiological model of morphological neuronal and glial plasticity in the adult hypothalamus. Front. Neuroendocrinol. *23*, 101–135.

Veenema, A.H., and Neumann, I.D. (2008). Central vasopressin and oxytocin release: regulation of complex social behaviours. Prog. Brain Res. *170*, 261–276.

Viviani, D., Charlet, A., van den Burg, E., Robinet, C., Hurni, N., Abatis, M., Magara, F., and Stoop, R. (2011). Oxytocin selectively gates fear responses through distinct outputs from the central amygdala. Science *333*, 104–107.

Wickersham, I.R., Lyon, D.C., Barnard, R.J., Mori, T., Finke, S., Conzelmann, K.K., Young, J.A., and Callaway, E.M. (2007). Monosynaptic restriction of transsynaptic tracing from single, genetically targeted neurons. Neuron *53*, 639–647.

Wickersham, I.R., Sullivan, H.A., and Seung, H.S. (2010). Production of glycoprotein-deleted rabies viruses for monosynaptic tracing and high-level gene expression in neurons. Nat. Protoc. *5*, 595–606.

Wilensky, A.E., Schafe, G.E., Kristensen, M.P., and LeDoux, J.E. (2006). Rethinking the fear circuit: the central nucleus of the amygdala is required for the acquisition, consolidation, and expression of Pavlovian fear conditioning. J. Neurosci. *26*, 12387–12396.

Wotjak, C.T., Ganster, J., Kohl, G., Holsboer, F., Landgraf, R., and Engelman, M. (1998). Dissociated central and peripheral release of vasopressin, but not oxytocin, in response to repeated swim stress: new insights into the secretory capacities of peptidergic neurons. Neuroscience *85*, 1209–1222.

Yizhar, O., Fenno, L.E., Davidson, T.J., Mogri, M., and Deisseroth, K. (2011). Optogenetics in neural systems. Neuron *71*, 9–34.

Zingg, H.H., and Lefebvre, D.L. (1988). Oxytocin and vasopressin gene expression during gestation and lactation. Brain Res. *464*, 1–6.